

Rotational Energy and the Diffuseness of the Boundary between Fusion and Strongly Damped Collisions

L. Adler, P. Gonthier, J. H. K. Ho,^(a) A. Khodai, M. N. Namboodiri, J. B. Natowitz, and S. Simon

Cyclotron Institute, Texas A&M University, College Station, Texas 77843

(Received 19 May 1980)

Differences in the kinetic energies of the fragments produced in the scission of the pairs of similar composite nuclei ^{59}Cu - ^{60}Zn and ^{83}Y - ^{88}Zr are interpreted as resulting from angular momentum fractionation. The energies indicate that some partial waves with angular momenta $10\hbar$ to $15\hbar$ below the sharp-cutoff fusion limit lead to strongly damped collisions.

PACS numbers: 25.70.Bc, 25.70.Fq, 25.70.Hi

Although the sharp-cutoff limiting angular momentum, L_c , is often used as a parameter to characterize the region of incident partial waves contributing to the fusion reaction, the actual boundary between fusion and nonfusion reactions may be quite diffuse.¹ Probing the competition between fusion and nonfusion reactions as a function of the incident partial wave can provide new insights into the mechanism of fusion. In this Letter, we show that comparisons of the measured kinetic energies of the products of completely damped collisions produced in the reactions of 150-MeV ^{20}Ne with ^{40}Ca , 214-MeV ^{32}S with ^{27}Al , 166-MeV ^{20}Ne with ^{63}Cu , and 237-MeV ^{40}Ar with Ti indicate that partial waves with angular momenta $10\hbar$ to $15\hbar$ below L_c contribute to strongly damped collisions.

A detector telescope placed at laboratory angles from 20° to 55° was used to detect and identify products of the reactions of 150-MeV ^{20}Ne with Ca and CaO, of 214-MeV ^{32}S with ^{27}Al , and of 237-MeV ^{40}Ar with Ti. The ΔE detector was a gas ionization chamber, 6 cm thick, operated at a pressure of 50 Torr P -10. A silicon detector 700 μm thick was used to measure the residual energy. Data were recorded eventwise. During analysis the energies of the Z identified products were corrected for energy losses in the target and detector window as well as for small pulse-height defects. For this purpose it was assumed $A = 2Z$. At the larger angles, the energy spectra of products ranging from $Z = 5$ to $Z = 20$ exhibited peaks characteristic of the deep-inelastic reaction mechanism. From these spectra the most probable energies were extracted for each detection angle. The observations on the CaO target were used to verify that the other data were free from significant oxygen contamination.

Again if we assume that $A = 2Z$, the most probable energies were transformed to the center of

mass. As the angle of observation increases, these most probable energies become constant within the experimental errors of ± 1 MeV. We take this constancy to be the signature of complete damping of the initial kinetic energy.

In Fig. 1, the most probable kinetic energies for the observed products of completely damped collisions, generally representing the average for two or more observation angles, are shown. The larger energies for the ^{88}Zr composite sys-

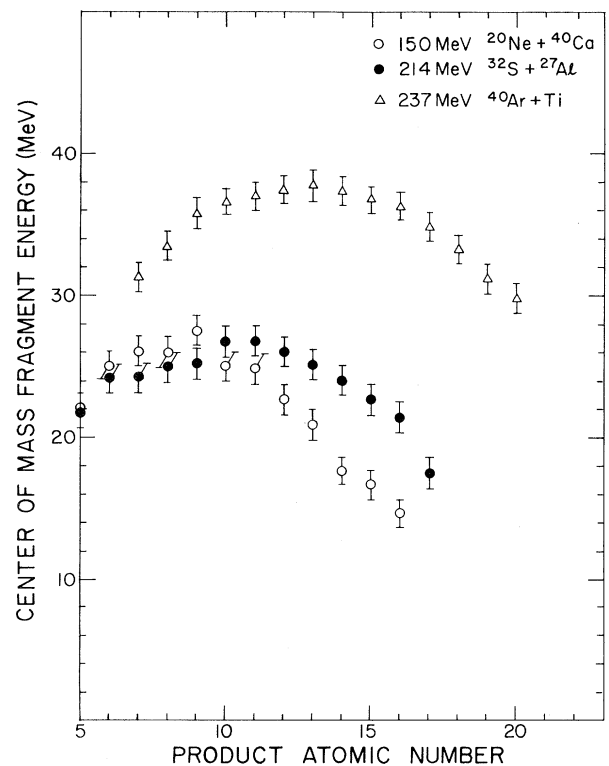


FIG. 1. Most probable fragment energies. The most probable kinetic energies in the center of mass are plotted for products of completely damped collisions.

tem are expected. However, the differences in the energies observed in the scission of the two essentially identical composite nuclei ^{59}Cu and ^{60}Zn are somewhat surprising. These differences are particularly large for products corresponding to near-symmetric breakup.

In fact, the choice of these two reaction systems was dictated by a desire on our part to match the important parameters of the ^{59}Cu and ^{60}Zn composite nuclei. The extent of this matching may be seen in Table I, where it can be noted that $E_{\text{c.m.}} - V$, the energy above the barrier in the center of mass, E_x , the excitation energy of the composite nucleus, L_g , the grazing angular momentum, and L_c , the sharp-cutoff limiting angular momentum, are almost identical for the two systems.

Apparently the entrance-channel asymmetry plays an important role in determining the properties of the completely damped scissioning nuclei. In the following we present arguments that the observed energy differences as well as similar differences between the $^{20}\text{Ne} + ^{63}\text{Cu}$ and $^{40}\text{Ar} + ^{48}\text{Ti}$ reactions result from angular momentum fractionation³ and more importantly, the data provide information on the diffuseness of the boundary between fusion and strongly damped collisions.

Several investigations indicate that complete damping leads to a deformed, rigidly rotating dinucleus.^{2,4,5} If the scission configuration is represented as two touching prolate spheroids the kinetic energy for scission is

$$E_K = Z_1 Z_2 e^2 / d + f^2 \hbar^2 l(l+1) / 2\mu d^2 + V_N, \quad (1)$$

where l is the initial partial wave, d is the internuclear distance, f is the ratio $\mu d^2 / (\mu d^2 + I_1 + I_2)$, and V_N is the nuclear potential.

For symmetric scission the liquid-drop model

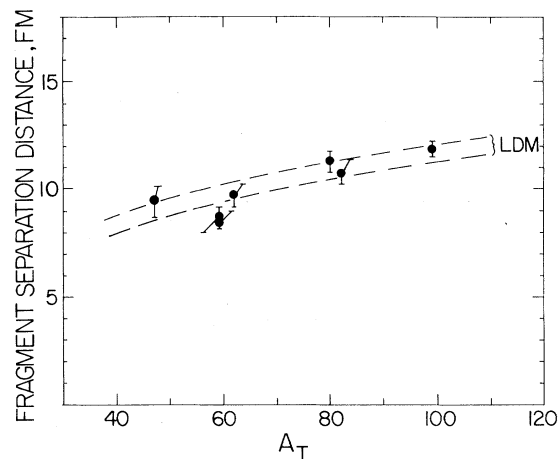


FIG. 2. Fragment separation distances for symmetric scission. The solid points represent distances derived from experimental energy measurements. The dashed lines indicate those calculated using the liquid-drop model with angular momenta ranging from 0 (lower limit) to the angular momentum at which $B_f = 0$ (upper limit).

(LDM)⁶ has been used to calculate saddle-point shapes and therefore d , as a function of angular momentum. The range of values thus calculated are presented in Fig. 2 for $0 \leq L \leq$ liquid-drop limit. For light nuclei the saddle-point shape should be a good approximation of the scission shape.

We have tested the LDM calculations for symmetric scission using data for systems where both the fragment kinetic energies and L_c are known.^{2,4,7-10} The observed energies and masses were corrected for evaporation effects and E_K was determined for the case in which two-body breakup was assumed. If we assume that the partial waves just above L_c lead to complete damp-

TABLE I. Energies and angular momentum limits for the systems discussed in the text.

Reaction	Composite nucleus	E_{lab} (MeV)	$E_{\text{c.m.}} - V$ (MeV)	E_x (MeV)	L_g^a (\hbar)	L_c (\hbar)
$^{20}\text{Ne} + ^{40}\text{Ca}$	^{60}Zn	150	67	109	59	49 ^b
$^{32}\text{S} + ^{27}\text{Al}$	^{59}Cu	214	64	111	59	49 ^b
$^{40}\text{Ar} + ^{48}\text{Ti}$	^{88}Zr	237	73	129	89	64 ^b
$^{20}\text{Ne} + ^{63}\text{Cu}$	^{83}Y	166	82	125	76	60

^a Classical calculation assuming $r = 1.44$.

^b Determined from systematics of experimental fusion cross-section measurements.

ing,^{2,4,5} the angular momentum was set to $L_c + 1$. Equation (1) was solved for d . For this purpose V_N was evaluated with use of the Bass potential.¹¹

The results appear in Fig. 2 as a function of the composite mass and show good agreement with the LDM calculations. Other values of L such that $(L_c + 1) \leq L \leq L_g$ lead to slightly higher values of d . Systems with large mass asymmetries in the entrance channel were not used for the test.

There is a model dependence in the determination of d by this method because the expression for E_K is double valued.¹² However, experiments in which both E_K and the intrinsic angular momentum are determined^{2,4,5} show clearly that the more deformed configuration is the correct one. It is this configuration we select. This selection is further supported by the excellent agreement indicated in Fig. 2.

No similar calculations exist for asymmetric scission configurations. We assume therefore that the effective radius parameters for asymmetric scission shapes are the same as those for symmetric scission shape of nuclei with the same composite mass. This assumption should introduce only small errors into the analysis.

To determine the range of partial waves contributing to completely damped collisions, (1) starting with $A = 2Z$ and the observed kinetic energy, we have used an iterative calculation to determine the average primary mass and kinetic energy; (2) we have used two-body kinematics to calculate the total kinetic energy E_K ; (3) we have used values of d derived from LDM calculations to calculate L using Eq. (1). This latter step also involves iteration since d varies slowly with L .

The results of the analysis for the reaction systems 214-MeV $^{32}\text{S} + ^{27}\text{Al}$ and 150-MeV $^{20}\text{Ne} + ^{40}\text{Ca}$ are presented in Fig. 3(a) where the extracted values of L are plotted against the primary-fragment atomic number. The dashed lines indicate the trend of the data. We see that the energy differences noted in Fig. 1 may be interpreted as resulting from the different angular momenta for the scissioning nuclei. Fragments with the projectile atomic number result from the highest partial waves while fragments with atomic numbers far removed from that of the projectile result from much lower partial waves, i.e., there is a significant angular momentum fractionation for the lower partial waves.

In Fig. 3(b) a similar analysis is shown for the reaction systems 166-MeV $^{20}\text{Ne} + ^{63}\text{Co}$ (Ref. 3) and 237 MeV $^{40}\text{Ar} + \text{Ti}$. Although not as well matched in their entrance channel parameters as the reac-

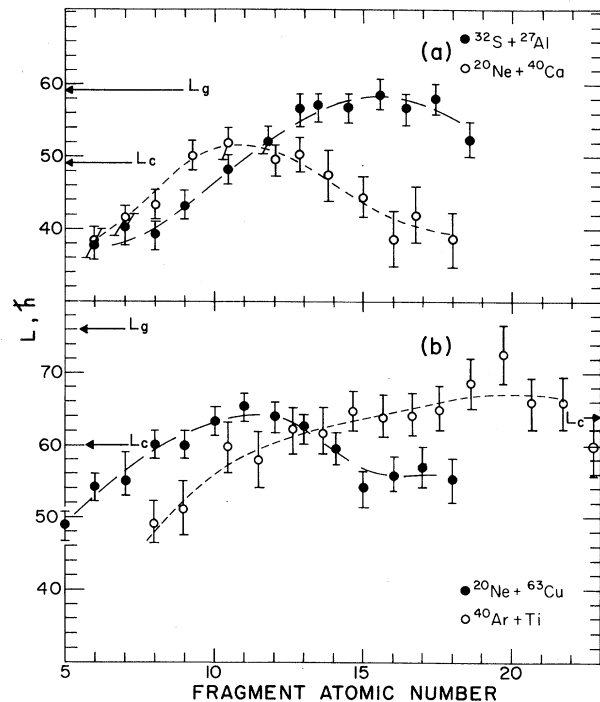


FIG. 3. Most probable values of L as a function of fragment atomic number. Values extracted from energy measurements (see text) for the similar composite systems ^{59}Cu and ^{60}Zn are shown in part (a). The grazing angular momentum L_g and sharp-cutoff limiting angular momentum L_c is the same for both systems. Data for the systems ^{83}Y and ^{88}Zr are shown in part (b). On the scale the values of L_g and L_c for the reaction $^{20}\text{Ne} + ^{63}\text{Cu}$ are indicated. On the right L_c for the reaction $^{40}\text{Ar} + \text{Ti}$ is shown. L_g for this system is $89\hbar$.

tions in 3(a), they are quite similar. The results of the analysis provide further evidence for large angular-momentum fractionation.

Recently, Simbel and Abul-Magd,¹³ using a somewhat different model, have arrived at a similar conclusion regarding angular momentum fractionation. In their model the angular momenta were constrained to be $\geq L_c$.

However, this work leads to the conclusion that the most probable angular momenta leading to products with atomic numbers far removed from the projectile are $10\hbar$ to $15\hbar$ lower than the sharp-cutoff angular momenta for the systems analyzed. This indicates that the boundary between fusion and strongly damped collisions is quite diffuse.

It is tempting to consider coupling this analysis with cross-section measurements to quantitatively determine the diffuseness of this boundary. To do so requires further information. The analysis applied here requires rigid rotation of the

system which is apparently not achieved prior to complete damping.^{2,5} Therefore only a portion of the cross section corresponds to this completely damped condition.

Finally we note that this analysis focusses only on the most probable partial waves. While in the classical model there is a correspondence between deflection angle and angular momentum, the experimental width of the energy distributions arises at least in part from the range of partial waves contributing to the observed products. Therefore partial waves even lower than those corresponding to the most probable kinetic energies can be contributing.

We appreciate useful conversations with C. Ngo, R. Schmitt, and J. M. Alexander. This research was supported by the U. S. Department of Energy and the Robert A. Welch Foundation. One of us (J. H. K. H.) is a recipient of a NATO Fellowship.

^(a)Present address: Max Planck Institute Kernphysik, Heidelberg, Germany.

¹D. Pelte and U. Smilansky, Phys. Rev. C **19**, 2196 (1979).

²R. A. Dayras *et al.*, to be published.

³M. M. Aleonard *et al.*, Phys. Rev. Lett. **40**, 622 (1978).

⁴D. Guerreau *et al.*, Brookhaven National Laboratory Report No. BNL-51115, 1979 (unpublished), Vol. 1, p. 59; R. Babinet *et al.*, to be published.

⁵M. N. Namboodiri *et al.*, Phys. Rev. C **20**, 982 (1979).

⁶S. Cohen *et al.*, Ann. Phys. (N.Y.) **82**, 557 (1974).

⁷T. M. Cormier *et al.*, Phys. Rev. C **16**, 215 (1977).

⁸J. B. Natowitz *et al.*, Nucl. Phys. **A277**, 477 (1977).

⁹B. Gatty *et al.*, Nucl. Phys. **A253**, 511 (1975).

¹⁰J. B. Natowitz *et al.*, Nukleonik **24**, 443 (1979).

¹¹R. Bass, Phys. Rev. Lett. **39**, 265 (1977).

¹²R. Betts and S. B. DiCenzo, Phys. Rev. C **19**, 2070 (1979).

¹³M. H. Simbel and A. Y. Abul-Magd, Z. Phys. A **294**, 277 (1980).

Observation of a $T_{>}$ Gamow-Teller State in $^{48}\text{Ca}(p,n)^{48}\text{Sc}$ at 160 MeV

B. D. Anderson, J. N. Knudson, P. C. Tandy, J. W. Watson, and R. Madey
Kent State University, Kent, Ohio 44242

and

C. C. Foster

Indiana University Cyclotron Facility, Bloomington, Indiana 47401
(Received 25 February 1980)

Neutron spectra from the reaction $^{48}\text{Ca}(p,n)^{48}\text{Sc}$ at 160 MeV reveal a prominent narrow peak at $E_x = 16.8$ MeV. This state is interpreted as a spin-flip isovector giant resonance; it carries a significant fraction of the $T_{>}$ ($T = 4$) Gamow-Teller strength. The observed position of this resonance agrees with both a recent shell-model prediction and with the position expected from systematics for the analog of the giant $M1$ resonance in ^{48}Ca .

PACS numbers: 24.30.Cz, 25.40.Ep, 27.40.+z

Broad peaks observed previously¹⁻⁴ in charge-exchange reactions on target nuclei with $N > Z$ were interpreted as carrying a significant amount of Gamow-Teller (spin-flip, isospin-flip) strength. The Gamow-Teller (GT) operator ($\sum_i \tau_i^- \vec{\sigma}_i$) acting on a target with $N > Z$ can populate states with isospin equal to ($T_{>}$) or one less than ($T_{<}$) the isospin of the target. (The GT operator can weakly excite states with isospin 1 greater than the isospin of the target.) The $T_{<}$ component of the GT strength was observed¹⁻⁴ via charge-exchange reactions in several nuclei to be broadly distributed near the isobaric analog state (IAS). The $T_{>}$ component of the GT strength is expected to appear at higher excitation energy. An earlier report² of $T_{>}$ GT strength in the reactions $^{90}\text{Zr}(p,$

$n)^{90}\text{Nb}$ and $^{90}\text{Zr}(^3\text{He}, t)^{90}\text{Nb}$ was reinterpreted⁵ as the $T_{<}$ component of the analog of the giant $E1$ resonance. In this Letter, we present neutron data showing a narrow (< 280 keV) state in the reaction $^{48}\text{Ca}(p,n)^{48}\text{Sc}$ at 160 MeV which we interpret as the $T_{>}$ ($T = 4$) component of the giant GT resonance in ^{48}Sc or equivalently as the analog of the giant $M1$ resonance in ^{48}Ca .

Neutron energy and angular distributions were measured by the time-of-flight technique at the beam-swinging facility⁶ of the Indiana University Cyclotron Facility. An energy resolution of 450 keV for 157-MeV neutrons was achieved with a flight path of 68.0 m. The neutron detector consisted of two large-volume (26.4-l) mean-timed,⁷ NE-102 plastic-scintillation counters preceded by